Supplementary Information: The quantification of amorphous phase content with the atomic pair distribution function

Joseph Peterson,[a] James TenCate,[b] Thomas Proffen,[c]
Timothy Darling,[d] Heinz Nakotte[a] and Katharine Page [e]*

[a]*Physics Department, New Mexico State University, P.O. Box 30001, Las Cruces, NM 88003 USA,* [b]*Earth and Environmental Science, Los Alamos National Laboratory, Los Alamos, NM 87545 USA,* [c]*Oak Ridge National Laboratory, Oak Ridge, TN 37831 USA,* [d]*Physics Department, University of Nevada, Reno, NV 89577 USA, and* [e]*Lujan Neutron Scattering Center, Los Alamos National Laboratory, Los Alamos, NM 87545 USA. E-mail: kpage@lanl.gov*

The following supplementary information includes details regarding data normalization, long-range structure refinement, and the model construction for crystalline quartz utilized in the article, *The quantification of amorphous phase content with the atomic pair distribution function.*

1. Data Normalization

Normalized total scattering patters, $S(Q)$, collected from NPDF with standard corrections applied for the two quartz samples and the five mixed samples are shown in Figure S1. In the transformation to real-space the following assumptions were made in the present study: (i) the coordination number of Si and the nearest-neighbor Si-O

atom-atom distribution is the same for all samples and (ii) the atomic number density is the same for all samples. These imply the first peak in each $G(r)$ should be identical. A multiplicative scale factor was calculated for each PDF to align the first peak in each dataset with the crushed glassy silica and then applied to the entire dataset range. This factor was needed to account for experimental differences in the sample volume in the neutron beam and the packing density of particles. The post scale factor PDFs for the mixed samples, the silica sample, the coarse quartz and the fine quartz are shown in Figure S2. The scale factors applied to each dataset are shown in Table S1.

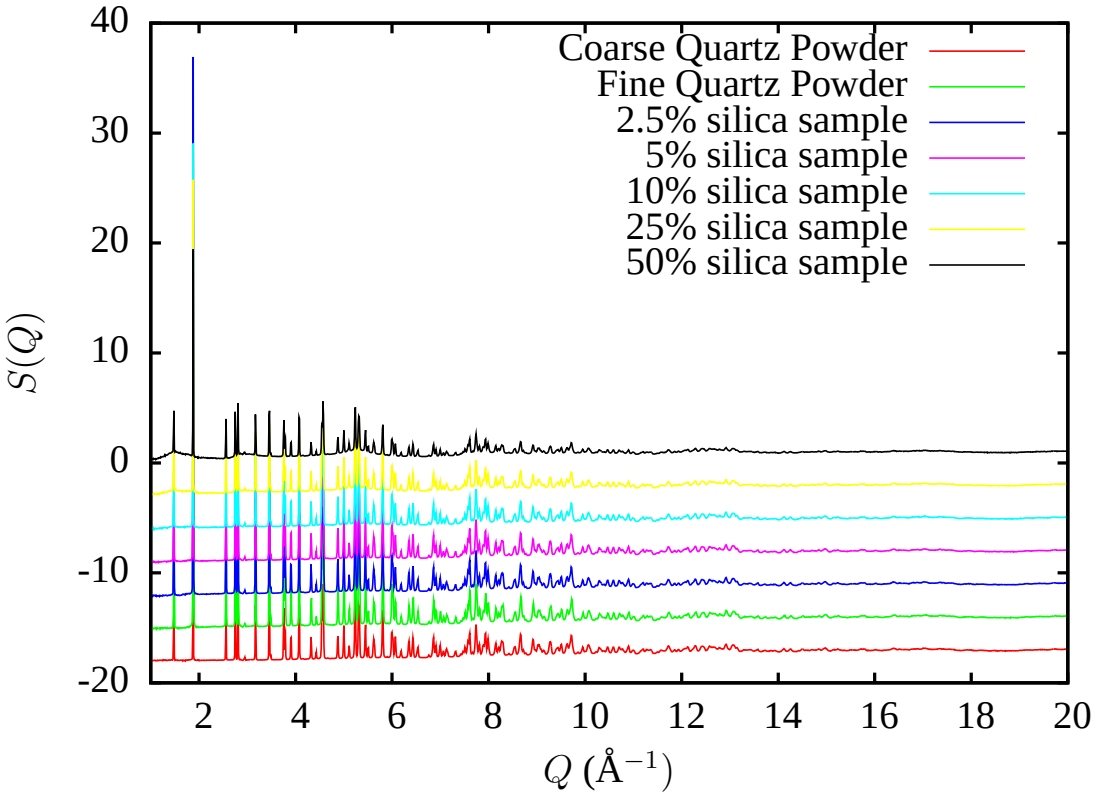

Fig. S1. Normalized total scattering pattern, $S(Q)$, for the mixed samples, fine quartz, and coarse quartz powder. An offset has been applied for clarity.

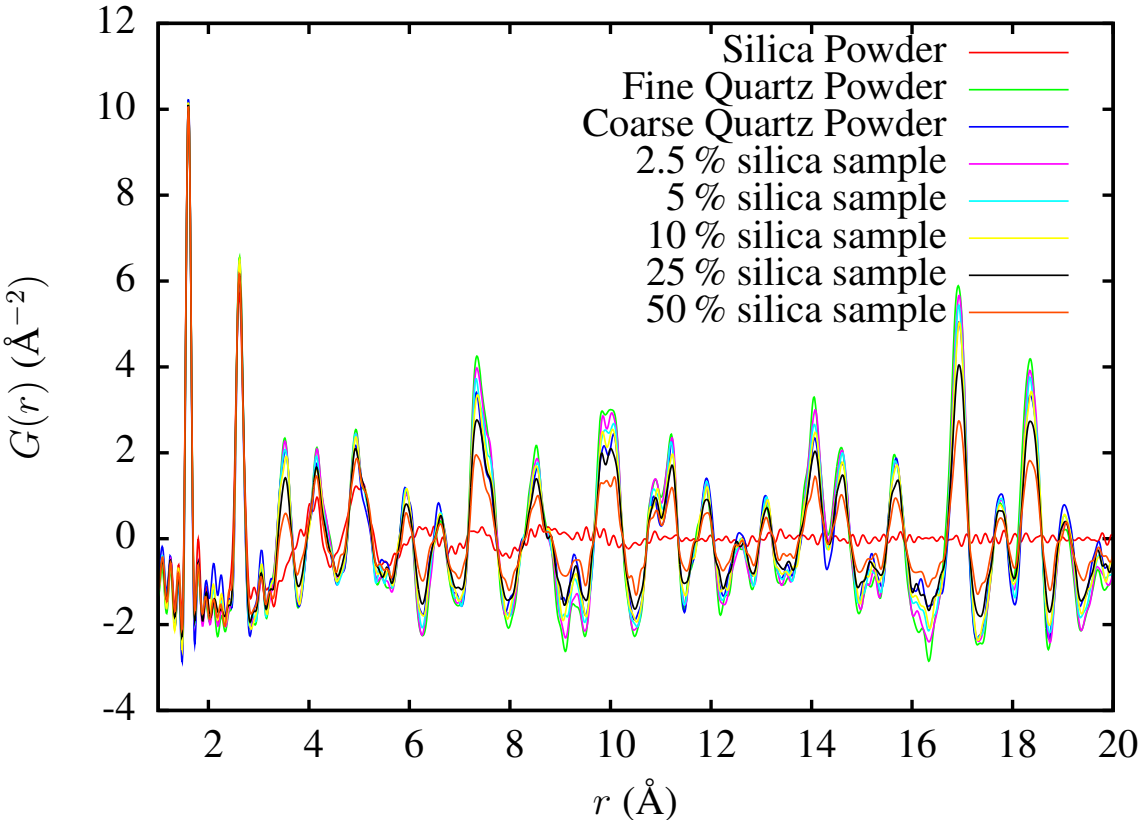

Fig. S2. Low-r region of the PDFs for the mixed samples, fine quartz, coarse quartz, and silica powder used in this study.

Table S1. *Scale Factors applied in each PDF to align first peaks.*

Sample	Scale Factor
2.5% silica	0.95862
5% silica	0.97654
10% silica	0.97101
25% silica	0.97062
50% silica	0.95544
Coarse quartz	1.0473
Fine quartz	0.93532

2. Long Range Structure Refinement

To model long-range behavior quantitatively and assure the purity of samples utilized, Rietveld analysis was conducted on each of the mixed sample and quartz datasets with the software package GSAS. In each case the 90, 119, and 148 degree banks from the

NPDF data were modeled with a crystalline quartz phase with space group $P3_121$ and lattice parameters $a = 4.91444$ and $c = 5.40646$. The refinement included the lattice parameters, the atomic positions, and the anisotropic atomic displacement parameters. The background for each dataset was fit with a fourth degree power series function. The same peak profile function was used in all refinements, though they were independently refined while the atomic displacement parameters were fixed. In all refinements except for the fine quartz the fits were significantly improved with the addition of primary extinction corrections. Best fits index all diffraction peaks and yield similar values for all parameters except primary extinction coefficients. Table S2 displays partial results of the analysis.

Table S2. *Partial results generated via Rietveld analysis for the various samples.*

Sample	Overall R_{wp} (%)	Average Primary Extinction Coeff. (μm^2)
2.5% silica	2.88 %	93.37
5% silica	2.81 %	237.89
10% silica	3.11%	220.21
25% silica	3.95%	237.77
50% silica	5.42%	269.82
Coarse quartz	2.76 %	754.59
Fine quartz	3.50 %	N/A

We specifically note that the same powder source was utilized to prepare all mixture samples. The difference we find in primary extinction coefficient across the series suggests that powder grains within the dynamical scattering regime were not evenly distributed among the samples.

3. Constructing a Model for Crystalline Quartz

Modeling the crystalline component of the mixed samples presented a challenge in this study. Distinct PDF peak intensity and shape were observed for samples with different degrees of dynamical scattering effects. Because dynamical scattering is currently not accounted for in PDF theory, directly generating a calculated model for real-space intensity is not possible.

To determine if the fine or coarse quartz could serve as a good model of crystalline behavior for our mixed standards, each mixed sample $G(r)$ was scaled to both the coarse and fine crystalline $G(r)$ in the 12 to 20 Å regime where there is no amorphous influence. In principal, if the long-range behavior is identical to either quartz model this scale factor multiplied by the fraction of crystalline content should be unity. As seen in Table S3 neither the coarse nor the fine quartz serve as an accurate model for the high-r behavior of the mixed samples. The mixed samples appear to have intermediate $G(r)$ behavior, consistent with their intermediate primary extinction correction found in Rietveld analysis. Recall above that powder grains within the dynamical scattering regime were not evenly distributed among the samples. This means that a single data set from the parent crystalline powder would not have been sufficient in modeling the crystalline phase in each of the mixtures. Thus the strategy implemented in the study utilized a combination of the coarse and fine data to construct a model for the crystalline phase in each separate case. This is presented in the main text.

Table S3. *Scale Factors (S.F.) required to match PDF data to coarse quartz data (left) and fine quartz data (right) in the 12 to 20 Å region. Also given is the ratio of Scale Factor to Crystalline Fraction (C.F.) for each dataset. A value of unity indicates a match to the longer range behavior.*

Sample	Fine Model		Coarse Model	
	S.F.	S.F. $*C.F$	S.F.	S.F. $*C.F.$
2.5% silica	1.0596	1.033	0.80178	0.7817
5% silica	1.1457	1.088	0.88085	0.8368
10% silica	1.2402	1.116	0.95356	0.8582
25% silica	1.4912	1.118	1.1446	0.8585
50% silica	2.2201	1.110	1.7018	0.8501

Also investigated was whether a properly normalized dataset of one of the mixed standards could be used as a model for the crystalline components of the data series. To do this the minimization scheme was modified to account for the amorphous fraction known to be present in the mixed standard used as a model with

$$G_{calc}(r) = x * G_{amorphous}(r) + \frac{1-x}{f}[G_{crystalline}(r) - (1-f)G_{amorphous}(r)] \qquad (1)$$

where x is the fraction of amorphous content and we again utilize a glassy silica dataset for $G_{amorphous}(r)$ and a mixed standard dataset as $G_{crystalline}(r)$. f is the known fraction of crystalline material in $G_{crystalline}(r)$ and it is assumed that $1 - f$ is the amorphous fraction in $G_{crystalline}(r)$ which can be modeled with $G_{amorphous}(r)$. Then a calculation can be preformed over all x to minimize

$$\sum_{i}^{N} [G_{sample}(r_i) - G_{calc}(r_i)]^2 \tag{2}$$

thus revealing the composition.

Table S4 shows the calculated amorphous content predicted for the standard samples utilizing each of the respective datasets as models in Equation (2), calculated over a 1 to 20 Å region. The table displays the poor performance of the minimizations utilizing the coarse or fine datasets as models of crystalline component. The results are improved utilizing the mixture datasets as models and the goodness of the model appears to be linked to how similar the primary extinction parameters are between the dataset used as a model and the dataset it is used to calculate.

Table S4. *Calculated amorphous percentages for a given sample (right column) given a crystalline basis (top row)*

Sample	Crystalline Model						
	Coarse	Fine	2.5%	5%	10%	25%	50%
2.5% silica	-16.6	7.0	*	-2.7	-4.9	-5.7	-4.6
5% silica	-7.9	14.8	10.8	*	3.2	2.6	4.3
10% silica	0.3	21.3	17.7	12.5	*	10.0	11.7
25% silica	17.5	34.7	31.5	27.3	25.7	*	26.6
50% silica	44.5	56.0	53.9	51.1	50.0	49.6	*